

## Monitoring Proton Release during Photosynthetic Water Oxidation in Photosystem II by Means of Isotope-Edited Infrared Spectroscopy

Hiroyuki Suzuki,<sup>†</sup> Miwa Sugiura,<sup>‡</sup> and Takumi Noguchi<sup>\*,†</sup>

*Institute of Materials Science, University of Tsukuba, Tsukuba, Ibaraki 305-8573, Japan, and Cell-Free Science and Technology Research Center, Ehime University, Matsuyama, Ehime 790-8577, Japan*

Received March 5, 2009; E-mail: tnoguchi@ims.tsukuba.ac.jp

**Abstract:** In photosynthetic water oxidation performed in the water oxidizing center (WOC) of photosystem II (PSII), two water molecules are converted into one oxygen molecule and four protons through a light-driven cycle of intermediates called S states ( $S_0$ – $S_4$ ). To understand the molecular mechanism of water oxidation and the chemical nature of substrate intermediates, it is essential to determine the stoichiometry of proton release from substrate water at individual S-state transitions. In this study, we have monitored proton release during water oxidation by means of isotope-edited Fourier transform infrared (FTIR) spectroscopy. FTIR difference spectra upon successive flash illumination were measured using PSII core complexes from a thermophilic cyanobacterium *Thermosynechococcus elongatus*, which were suspended in a high concentration (200 mM) Mes buffer at pH 6.0. The spectra involved, in addition to protein bands, the bands of the Mes buffer that trapped virtually all protons from the WOC. Mes-only signals were extracted by subtracting the spectra measured in deuterated-Mes (Mes- $d_{12}$ ). The flash-number dependence of the intensity increase of the isotope-edited Mes signal showed a clear period-four oscillation. By simulating the oscillation with different assumptions about miss factors, the proton release pattern was estimated to be 0.8–1.0:0.2–0.3:0.9–1.2:1.5–1.6 for the  $S_0$ → $S_1$ → $S_2$ → $S_3$ → $S_0$  transitions. The effect of H/D exchange on the COOH region of proteins in FTIR difference spectra of the S-state cycle showed that protonation/deprotonation of carboxylic groups contributed little to the observed proton release pattern. Together with the present and previous FTIR results suggesting no involvement of also His and Cys side groups, it was concluded that proton release from substrate water takes place with a 1:0:1:2 stoichiometry, which is perturbed by partial protonation/deprotonation of side groups probably of Arg, Lys, or Tyr located nearby the WOC.

### Introduction

Photosynthetic oxygen evolution performed by plants and cyanobacteria provides oxygen in the atmosphere, which sustains life on the earth. In this process, molecular oxygen is generated by oxidation of water at the water-oxidizing center (WOC) in photosystem II (PSII),<sup>1–4</sup> and electrons abstracted from water are used ultimately to reduce CO<sub>2</sub> and produce sugars. The WOC consists of a metal cluster of four Mn ions and one Ca<sup>2+</sup>, called the Mn cluster, and surrounding amino acid ligands, embedded in PSII protein complexes.<sup>5–7</sup>

The reaction proceeds via a light-driven cycle of five intermediates ( $S_i$  states;  $i = 0–4$ ), the so-called S-state cycle, in which two water molecules are converted into one molecular oxygen and four protons.<sup>1–4</sup> Among the five intermediates, the  $S_1$  state is the most stable in the dark, and repetitive flash illumination advances each S state to the next state forming a cycle:  $S_1$ → $S_2$ → $S_3$ → $S_0$ → $S_1$ . Molecular oxygen is released during the  $S_3$ → $S_0$  transition via the transient  $S_4$  state. Details of the molecular mechanism of water oxidation, however, remain largely unknown.

Monitoring protons liberated from substrate water and determining the proton release stoichiometry for individual S-state transitions are essential for understanding the molecular mechanism of water oxidation and the chemical nature of substrate intermediates at each S state. Experimental efforts to detect proton release have been made by measuring flash-induced pH changes using pH-indicating dyes and a sensitive pH electrode.<sup>8–11</sup> The 1:0:1:2 pattern for the  $S_0$ → $S_1$ → $S_2$ →

<sup>†</sup> University of Tsukuba.

<sup>‡</sup> Ehime University.

- (1) Debus, R. J. *Biochim. Biophys. Acta* **1992**, *1102*, 269–352.
- (2) Hillier, W.; Messinger, J. In *Photosystem II: The Light-Driven Water: Plastoquinone Oxidoreductase*; Wydrzynski, T., Satoh, K., Eds.; Springer: Dordrecht, The Netherlands, 2005; pp 567–608.
- (3) McEvoy, J. P.; Brudvig, G. W. *Chem. Rev.* **2006**, *106*, 4455–4483.
- (4) Renger, G. *Photosynth. Res.* **2007**, *92*, 407–425.
- (5) Ferreira, K. N.; Iverson, T. M.; Maghlaoui, K.; Barber, J.; Iwata, S. *Science* **2004**, *19*, 1831–1838.
- (6) Loll, B.; Kern, J.; Saenger, W.; Zouni, A.; Biesiadka, J. *Nature* **2005**, *438*, 1040–1044.
- (7) Yano, J.; Kern, J.; Sauer, K.; Latimer, M. J.; Pushkar, Y.; Biesiadka, J.; Loll, B.; Saenger, W.; Messinger, J.; Zouni, A.; Yachandra, V. K. *Science* **2006**, *314*, 821–825.

(8) Lavergne, J.; Junge, W. *Photosynth. Res.* **1993**, *38*, 279–296.

(9) Haumann, M.; Junge, W. In *Oxygenic Photosynthesis: The Light Reactions*; Ort, D. R., Yocum, C. F., Eds.; Kluwer Academic Publishers: Dordrecht, The Netherlands, 1996; Vol. 4, pp 165–192.

S<sub>3</sub>→S<sub>0</sub> transitions was first widely accepted by experiments using thylakoids.<sup>12–14</sup> However, it was later found that the proton pattern is generally a noninteger and strongly dependent on pH, materials, and even the presence of glycerol.<sup>8–11,14–23</sup> In particular, PSII core complexes from higher plants in a medium without glycerol showed an approximate 1:1:1:1 pattern.<sup>15,20,22</sup> Some models of the water oxidation mechanism were based on this simple pattern adopted as the proton release stoichiometry from substrate water, while some other models adopted the original 1:0:1:2 pattern.<sup>2,3</sup> The controversial proton patterns have been ascribed to the electrostatically driven proton release/uptake of amino acid groups at the peripheral, which can be different between materials.<sup>8–11,24</sup> However, these amino acid groups participating in proton release have not been identified yet, and hence conclusions on the pattern of proton release from substrate water and the mechanism of showing different apparent proton patterns have yet to be reached.

In the previous proton release experiments, pH shifts were usually monitored in media with a very low concentration buffer or even without buffer.<sup>17–23</sup> In such a low concentration buffer, however, there is a concern that protons released from WOC are trapped by PSII proteins that possess a large number of protonatable groups, and that the protonation of side groups could in turn affect the PSII reactions. In addition, in many of previous proton release measurements, artificial quinones are used as electron acceptors, which could disturb the apparent proton release pattern by proton uptake upon their reduction. There is also a possibility that peripheral cofactors such as the nonheme iron and Y<sub>D</sub>, which undergo proton release or uptake upon their photoreactions,<sup>25,26</sup> contribute to the proton release pattern.

Light-induced FTIR difference spectroscopy has been used as a powerful method to investigate the molecular mechanisms of electron transfer and water oxidation reactions in PSII.<sup>27–31</sup> FTIR spectra of individual redox cofactors can be obtained by

changing measurement conditions, and the structures and reactions of the cofactor sites including amino acid side chains and water molecules can be studied.<sup>27</sup> As for the WOC, FTIR difference spectra of individual S-state transitions have been measured by applying successive flashes.<sup>32,33</sup> Information on the core structure of the Mn cluster,<sup>34</sup> its carboxylate and His ligands,<sup>35–42</sup> and the reactions of substrate water<sup>31,43–45</sup> have been obtained.

In this study, we have monitored proton release during photosynthetic water oxidation by means of isotope-edited FTIR difference spectroscopy. The concept of proton detection by this method is (1) trapping all protons released from the WOC using a high concentration buffer, (2) detecting buffer reactions using light-induced FTIR difference spectroscopy, (3) obtaining buffer-only signals without protein contributions using isotope-labeled buffer molecules, and (4) estimating the proton release from flash-dependent intensity changes of the buffer signals. As a sample for this experiment, we used very stable PSII core complexes from a thermophilic cyanobacterium *Thermosynechococcus elongatus*,<sup>46</sup> which have been used for X-ray crystallographic studies,<sup>5,6,47</sup> and also as an electron acceptor, ferricyanide was used, instead of artificial quinones, to avoid proton uptake on the electron acceptor side. Merits of this proton detection method over the previous methods are that (1) the amount of released protons can be accurately estimated without interference of buffering function of proteins; (2) the pH change during measurements is kept minimal, which could otherwise affect the reactions in the WOC; (3) simultaneous detection of S-state cycling can be achieved using the oscillation of protein bands, whereas parallel experiments of flash-induced O<sub>2</sub> evolution or UV detection were necessary in the previous methods;<sup>17,19–21</sup> (4) information on the protonation/deprotonation of amino acid groups can be directly obtained; (5) reactions of other cofactors such as the nonheme iron and Y<sub>D</sub>, which can disturb the proton pattern, can be simultaneously monitored; and (6) infrared light as measuring light does not affect the photoreaction, which is in contrast to the experiments using visible light to detect absorption changes of pH-indicating dyes. The obtained results strongly support the view that protons are

- (10) Junge, W.; Haumann, M.; Ahlbrink, R.; Mulikidjanian, A.; Clausen, J. *Philos. Trans. R. Soc. London, Ser. B* **2002**, 357, 1407–1417.
- (11) Rappaport, F.; Lavergne, J. *Biochim. Biophys. Acta* **2001**, 1503, 246–259.
- (12) Fowler, C. F. *Biochim. Biophys. Acta* **1977**, 462, 414–421.
- (13) Saphon, S.; Crofts, A. R. Z. *Naturforsch.* **1977**, 32C, 617–626.
- (14) Förster, V.; Junge, W. *Photochem. Photobiol.* **1985**, 41, 183–190.
- (15) Wacker, U.; Haag, E.; Renger, G. In *Current Research in Photosynthesis*; Baltscheffsky, M., Ed.; Kluwer: Dordrecht, 1990; Vol. 1, pp 869–872.
- (16) Lavergne, J.; Rappaport, F. In *Current Research in Photosynthesis*; Baltscheffsky, M., Ed.; Kluwer: Dordrecht, 1990; Vol. 1, pp 873–876.
- (17) Rappaport, F.; Lavergne, J. *Biochemistry* **1991**, 30, 10004–10012.
- (18) Jahns, P.; Lavergne, J.; Rappaport, F.; Junge, W. *Biochim. Biophys. Acta* **1991**, 1057, 313–319.
- (19) Jahns, P.; Junge, W. *Biochemistry* **1992**, 31, 7398–7403.
- (20) Lübbers, K.; Haumann, M.; Junge, W. *Biochim. Biophys. Acta* **1993**, 1183, 210–214.
- (21) Haumann, M.; Junge, W. *Biochemistry* **1994**, 33, 864–872.
- (22) Haumann, M.; Hundelt, M.; Jahns, P.; Chroni, S.; Bögershausen, O.; Ghanotakis, D.; Junge, W. *FEBS Lett.* **1997**, 410, 243–248.
- (23) Schlodder, E.; Witt, H. T. *J. Biol. Chem.* **1999**, 274, 30387–30392.
- (24) Renger, G. *Photosynthetica* **1987**, 21, 203–224.
- (25) Berthomieu, C.; Hienerwadel, R. *Biochemistry* **2001**, 40, 4044–4052.
- (26) Hienerwadel, R.; Gourion-Arsiquaud, S.; Ballottari, M.; Bassi, R.; Diner, B. A.; Berthomieu, C. *Photosynth. Res.* **2005**, 84, 139–144.
- (27) Noguchi, T.; Berthomieu, C. *Photosystem II: The Light-Driven Water: Plastocyanin Oxidoreductase*; Wydrzynski, T., Satoh, K., Eds.; Springer: Dordrecht, The Netherlands, 2005; pp 367–387.
- (28) Noguchi, T. *Photosynth. Res.* **2007**, 91, 59–69.
- (29) Noguchi, T. *Coord. Chem. Rev.* **2008**, 252, 336–346.
- (30) Debus, R. J. *Coord. Chem. Rev.* **2008**, 252, 244–258.
- (31) Noguchi, T. *Philos. Trans. R. Soc. London, Ser. B* **2008**, 363, 1189–1195.

- (32) Noguchi, T.; Sugiura, M. *Biochemistry* **2001**, 40, 1497–1502.
- (33) Hillier, W.; Babcock, G. T. *Biochemistry* **2001**, 40, 1503–1509.
- (34) Chu, H.-A.; Sackett, H.; Babcock, G. T. *Biochemistry* **2000**, 39, 14371–14376.
- (35) Noguchi, T.; Ono, T.; Inoue, Y. *Biochim. Biophys. Acta* **1995**, 1228, 189–200.
- (36) Noguchi, T.; Inoue, Y.; Tang, X.-S. *Biochemistry* **1999**, 38, 10187–10195.
- (37) Suzuki, H.; Taguchi, Y.; Sugiura, M.; Boussac, A.; Noguchi, T. *Biochemistry* **2006**, 45, 13454–13464.
- (38) Kimura, Y.; Mizusawa, N.; Yamanari, T.; Ishii, A.; Ono, T. *J. Biol. Chem.* **2005**, 280, 2078–2083.
- (39) Kimura, Y.; Mizusawa, N.; Ishii, A.; Ono, T. *Biochemistry* **2005**, 44, 16072–16078.
- (40) Chu, H.-A.; Hillier, W.; Debus, R. J. *Biochemistry* **2004**, 43, 3152–3166.
- (41) Debus, R. J.; Strickler, M. A.; Walker, L. M.; Hillier, W. *Biochemistry* **2005**, 44, 1367–1374.
- (42) Strickler, M. A.; Walker, L. M.; Hillier, W.; Britt, R. D.; Debus, R. J. *Biochemistry* **2007**, 46, 3151–3160.
- (43) Noguchi, T.; Sugiura, M. *Biochemistry* **2000**, 39, 10943–10949.
- (44) Noguchi, T.; Sugiura, M. *Biochemistry* **2002**, 41, 15706–15712.
- (45) Suzuki, H.; Sugiura, M.; Noguchi, T. *Biochemistry* **2008**, 47, 11024–11030.
- (46) Sugiura, M.; Inoue, Y. *Plant Cell Physiol.* **1999**, 40, 1219–1231.
- (47) Murray, J. W.; Maghlaoui, K.; Kargul, J.; Ishida, N.; Lai, T.-L.; Rutherford, A. W.; Sugiura, M.; Boussac, A.; Barber, J. *Energy Environ. Sci.* **2008**, 1, 161–166.

released from substrate water with a 1:0:1:2 pattern for the S<sub>0</sub>→S<sub>1</sub>→S<sub>2</sub>→S<sub>3</sub>→S<sub>0</sub> transitions.

## Materials and Methods

**Samples.** The PS II core complexes from the *T. elongatus* 43-H strain, in which the carboxyl terminus of the CP43 subunit was genetically histidine-tagged, were purified using Ni<sup>2+</sup>-affinity column chromatography as described previously.<sup>46</sup> The buffer was once exchanged to 1 mM 2-(*N*-morpholino)ethanesulfonic acid (Mes) (pH 6.0) containing 5 mM NaCl, 5 mM CaCl<sub>2</sub>, and 0.06% *n*-dodecyl β-D-maltoside using Microcon-100 (Amicon), and the core complexes were concentrated to 10 mg of Chl/mL. An aliquot (1.5 μL) of this sample and an equivalent volume of a 100 mM potassium ferricyanide solution were deposited on a CaCl<sub>2</sub> plate (25 mm in diameter) and lightly dried under N<sub>2</sub> gas. The sample was then mixed with 1.5 μL of a 200 mM Mes or Mes-*d*<sub>12</sub> buffer (pH 6.0) containing 5 mM NaCl, 5 mM CaCl<sub>2</sub>, 100 mM potassium ferricyanide, and 0.06% *n*-dodecyl β-D-maltoside (final core concentration: 10 mg of Chl/mL), and this solution was sandwiched with another CaF<sub>2</sub> plate with a circular groove (14 mm inner diameter; 1 mm width).<sup>32</sup> The Mes-*d*<sub>12</sub> buffer was prepared by dissolving Mes-*d*<sub>13</sub> (Cambridge Isotope Laboratories, Inc., 98% D) in H<sub>2</sub>O, where the sulfonic acid group is ionized. The sample cell was sealed with silicone grease in the outer part of the groove, where a tiny piece of aluminum foil was placed as a spacer. In this cell, the absorbance of a 1651 cm<sup>-1</sup> peak consisting of water HOH bending and amide I bands was kept at ~1. The sample temperature was maintained at 10 °C by circulating cold water in a copper holder. The sample was stabilized for 12 h in the dark before starting measurement.

**FTIR Measurements.** Flash-induced FTIR difference spectra were measured on a Bruker IFS-66/S spectrophotometer equipped with an MCT detector (InfraRed D316/8) at 4 cm<sup>-1</sup> resolution.<sup>28</sup> Flash illumination was performed by a Q-switched Nd:YAG laser (Quanta-Ray GCR-130, 532 nm, ~7 ns fwhm, ~7 mJ cm<sup>-1</sup> pulse<sup>-1</sup> at the sample point). The PSII core sample was illuminated by two preflashes (1 s interval) followed by dark adaptation for 30 min to synchronize all the centers to the S<sub>1</sub> state. Twelve flashes were then applied to the sample at intervals of 20 s, and single-beam spectra (20-s scan) were measured before the first flash, between the flashes, and after the 12th flash. The sample was then dark adapted for 30 min again. This entire process was repeated six times, and the spectra were averaged to calculate flash-induced difference spectra. Spectra were measured using four different samples to obtain final average data.

The COOH region (1760–1700 cm<sup>-1</sup>) of flash-induced spectra of the S-state cycle in 200 mM Mes/H<sub>2</sub>O and Mes/D<sub>2</sub>O buffers (pH(D) 6.0) was measured using a core sample at a doubled concentration to achieve a higher S/N ratio. Four successive flashes, instead of 12 flashes, were applied to the sample, and measurements were repeated 24 times keeping other conditions of preflash illumination and dark adaptation identical to those of the above measurements. Because of this repetitive S-state cycling, a long incubation in the Mes/D<sub>2</sub>O buffer for H/D exchange was unnecessary; protons that undergo release or uptake during the cycle are exchanged to deuterons in the first cycle. One sample was used for each measurement in the Mes/H<sub>2</sub>O or Mes/D<sub>2</sub>O buffer.

FTIR spectra of aqueous solutions of a Mes and ferricyanide mixture were measured between a pair of BaF<sub>2</sub> plates at room temperature. The CN band of ferricyanide was used as an internal standard rather than that of ferrocyanide with a much stronger intensity, because the latter CN band was significantly broadened or shifted in acidic solutions, whereas the ferricyanide CN band was not. For protonated Mes, an acidic solution (pH 3.0) involving 100 mM Mes (or Mes-*d*<sub>12</sub>), 100 mM potassium ferricyanide, and 1 mM HCl was used, while, for deprotonated Mes, an alkaline solution (pH 11.9) involving the same amount of Mes and potassium ferricyanide together with 110 mM NaOH was used. With a p*K*<sub>a</sub>

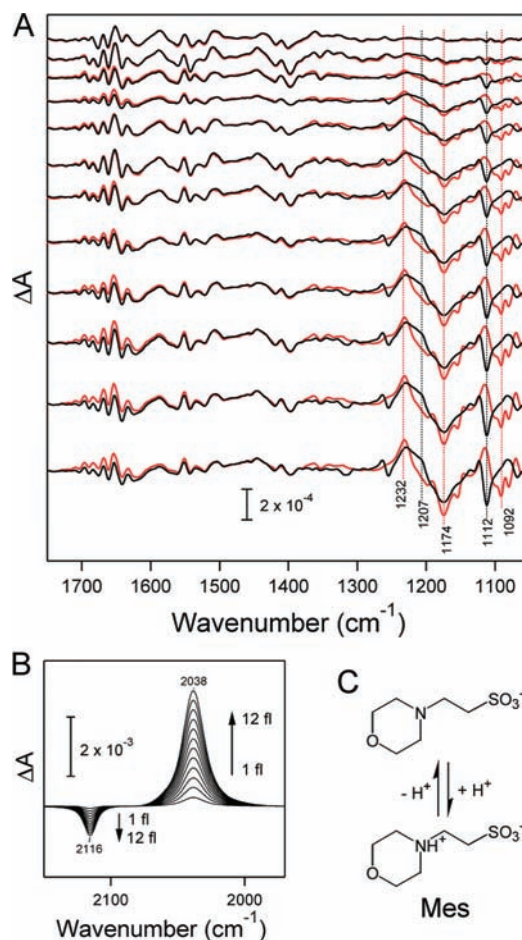


**Figure 1.** (A) FTIR difference spectra (1750–1050 cm<sup>-1</sup>) upon successive flash illumination on the PSII core complexes from *T. elongatus* in unlabeled Mes (black lines) and Mes-*d*<sub>12</sub> (red lines) buffers (pH 6.0) at a 200 mM concentration. Difference spectra were calculated between the spectra recorded before illumination and after the *n*th flash (*n* = 1–12, from top to bottom). (B) The CN stretching region of ferricyanide (2116 cm<sup>-1</sup>) and ferrocyanide (2038 cm<sup>-1</sup>) of the FTIR difference spectra (*n*th flash - minus-before illumination) in an unlabeled Mes buffer. (C) Chemical structures of the protonated and deprotonated forms of Mes.

of 6.15, more than 99% of Mes is protonated and deprotonated in the former and latter solutions, respectively.

FTIR spectra of aqueous solutions (in H<sub>2</sub>O and D<sub>2</sub>O) of a propionic acid and ferricyanide mixture were also measured at room temperature. The solution involved 150 mM propionic acid and 15 mM potassium ferricyanide, showing a pH of 2.7. With a p*K*<sub>a</sub> of 4.88, more than 99% of propionic acid takes a protonated form.

**Fitting Analysis.** Spectral fitting and simulations of oscillation patterns were performed using Igor Pro.Ver5 (WaveMetrics Inc., Lake Oswego, U.S.A.).

## Results

### FTIR Difference Spectra of PSII during Water Oxidation

**by Successive Flashes.** Figure 1A (black lines) shows FTIR difference spectra upon successive flash illumination on the PSII core complexes in a Mes (Figure 1C) buffer (pH 6.0) at a relatively high concentration (200 mM). The spectra represent differences between before illumination and after the *n*th flash (*n* = 1–12: from top to bottom). The sample involved ferricyanide as an exogenous electron acceptor, and its reduction on the electron acceptor side was expressed as negative/positive peaks at 2116/2038 cm<sup>-1</sup> arising from the CN stretching bands of ferricyanide/ferrocyanide (Figure 1B). The observed stepwise

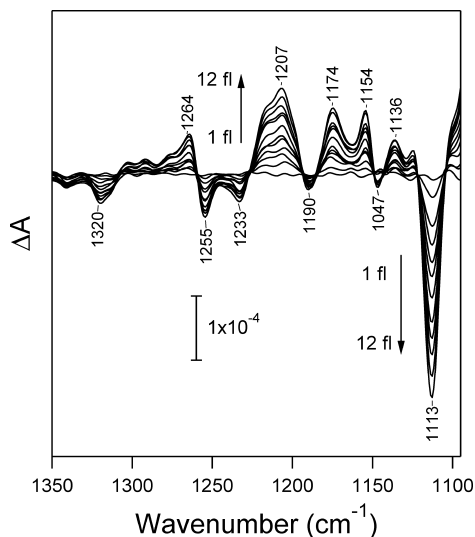


**Figure 2.** Mes-minus-Mes- $d_{12}$  double difference spectra of the flash-induced difference spectra ( $n$ th flash-minus-before illumination;  $n = 1-12$ ), representing Mes signals without protein bands.

increase of this ferricyanide/ferrocyanide signal indicates that electrons flow smoothly in PSII during measurements.

On the electron donor side, electrons are withdrawn from the WOC and eventually from water molecules via S-state cycling. Because both ferricyanide and ferrocyanide do not show bands in the frequency region of Figure 1A (1750–1050  $\text{cm}^{-1}$ ), spectra in this region express the events that took place in the WOC. Previous studies using isotope substitution have shown that bands at 1700–1600, 1600–1450, and 1450–1350  $\text{cm}^{-1}$  typically represent the amide I, amide II/asymmetric  $\text{COO}^-$ , and symmetric  $\text{COO}^-$  vibrations, respectively,<sup>48,49</sup> which reflect the structural changes of the protein moiety around the Mn cluster and its amino acid ligands from the initial  $S_1$  state to the  $S_i$  states ( $i = 0-3$ ) distributed after flash illumination.

In addition to these protein bands, several prominent bands were observed in the 1300–1050  $\text{cm}^{-1}$  region. Since these bands increased their intensities as the flash number increases, they are not attributed to the proteins but probably to the Mes molecules that trapped protons released from the WOC. This idea was confirmed by similar measurements in a buffer of Mes- $d_{12}$ , in which all nonexchangeable hydrogens are replaced with deuteriums (see the Mes structure in Figure 1C). In this isotope-labeled buffer, bands at 1300–1050  $\text{cm}^{-1}$  were significantly altered (Figure 1A, red lines), whereas other bands at 1700–1350  $\text{cm}^{-1}$  were virtually unchanged.

To accurately estimate the intensities of the Mes bands in the difference spectra, double difference spectra as Mes-minus-Mes- $d_{12}$  were calculated to delete the protein bands, some of which overlapped the Mes region. The subtraction factor was determined so as to cancel the symmetric  $\text{COO}^-$  region (1450–1350  $\text{cm}^{-1}$ ) of the first-flash spectra, in which the Mes contribution was trivial. The resultant isotope-edited double difference spectra are presented in Figure 2. The spectra consist of only the Mes vibrations and thus eventually represent the amount of protons liberated from the WOC during water oxidation. The signals increased with the flash number, indicat-

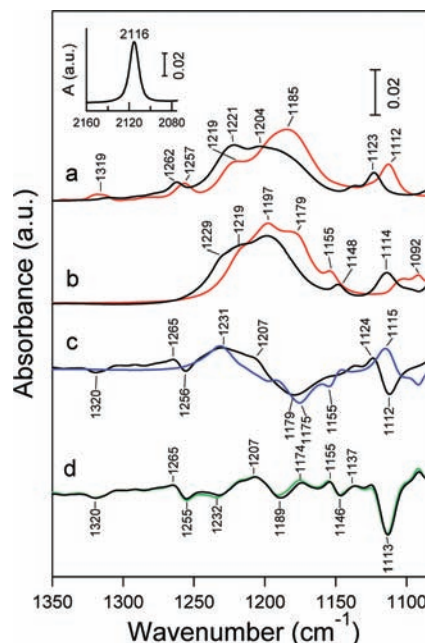


**Figure 3.** FTIR spectra of Mes solutions (100 mM) in the presence of ferricyanide (100 mM). (a) Unlabeled Mes in protonated (black line) and deprotonated (red line) forms. The inset shows the CN stretching band of ferricyanide in the protonated Mes solution. (b) Mes- $d_{12}$  in protonated (black line) and deprotonated (red line) forms. Spectra in panels a and b were scaled so as to match the CN peak intensity to that of protonated Mes (inset). (c) Protonated-minus-deprotonated difference spectra of Mes (black line) and Mes- $d_{12}$  (blue line). (d) Mes-minus-Mes- $d_{12}$  double difference spectrum of protonated-minus-deprotonated difference spectra (black line) in comparison with the corresponding double difference spectrum of PSII upon 12 flash illumination. The latter spectrum was scaled with a factor to match the intensity of the ferricyanide peak at 2116  $\text{cm}^{-1}$  of the 12 flash-induced difference spectrum (Figure 1B, the largest spectrum) and that of the Mes and ferricyanide solution (panel a, inset).

ing that protons were continuously released into the bulk and trapped by Mes molecules.

**FTIR Spectra of Mes Solutions.** For further identification of the Mes bands and estimation of the amount of protons released from PSII, FTIR spectra of Mes solutions (100 mM) in the presence of equimolar ferricyanide (100 mM) were measured (Figure 3). Unlabeled Mes (Figure 3a) and Mes- $d_{12}$  (Figure 3b) in protonated (black lines) and deprotonated (red lines) forms show prominent bands in the frequency region below 1300  $\text{cm}^{-1}$ . Spectra were scaled on the CN band of ferricyanide (inset). Group frequencies<sup>50</sup> and our preliminary vibrational analyses using Hartree–Fock calculations indicated that strong bands at 1250–1150  $\text{cm}^{-1}$  and medium bands at 1125–1090  $\text{cm}^{-1}$  arise from the asymmetric  $\text{SO}_3$  stretching and morpholino ring vibrations, respectively, both of which are coupled with the  $\text{CH}_2$  deformations of the side chain.

Difference spectra between the deprotonated and protonated forms (protonated-minus-deprotonated) of Mes (Figure 3c, black line) and Mes- $d_{12}$  (Figure 3c, blue line) were very similar to the spectral features in the 1300–1050  $\text{cm}^{-1}$  region in the flash-induced FTIR difference spectra of PSII in 200 mM Mes and Mes- $d_{12}$  buffers, respectively (Figure 1A). The Mes-minus-Mes- $d_{12}$  double difference spectrum of the protonated-minus-deprotonated spectra (Figure 3d, black line) showed features virtually identical to the corresponding double difference spectrum of

(48) Noguchi, T.; Sugiura, M. *Biochemistry* **2003**, *42*, 6035–6042.

(49) Yamanari, T.; Kimura, Y.; Mizusawa, N.; Ishii, A.; Ono, T. *Biochemistry* **2004**, *43*, 7479–7490.

(50) Socrates, G. *Infrared characteristic group frequencies*; John Wiley & Sons: Chichester, 1994.

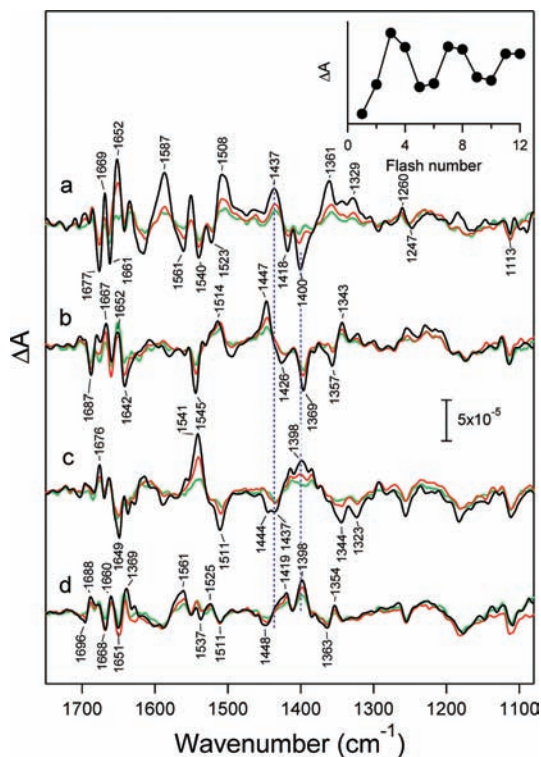


**Figure 4.** FTIR difference spectra of the S-state cycle upon individual flashes. The difference spectra were calculated between before and after the  $n$ th flash ( $n = 1-4$ ; black lines,  $n = 5-8$ ; red lines,  $n = 9-12$ ; green lines). (a) 1st, 5th, and 9th flash; (b) 2nd, 6th, and 10th flash; (c) 3rd, 7th, and 11th flash; (d) 4th, 8th, and 12th flash. The inset shows the oscillation pattern of the protein bands estimated by the intensity difference at 1437 and 1400  $\text{cm}^{-1}$  in the symmetric carboxylate stretching region (dotted blue lines).

PSII upon 12 flash illumination (Figure 3d, green line). The latter spectrum was scaled with a factor to match the ferricyanide peak at 2116  $\text{cm}^{-1}$  of the 12 flash-induced difference spectrum of PSII (Figure 1B, largest spectrum) to that of the Mes and ferricyanide solution (Figure 3a, inset). The intensity of this PSII spectrum was almost identical to that of the Mes solution (Figure 3d), indicating that the same number of Mes molecules reacted as that of ferricyanide upon illumination on the PSII core complexes. In other words, on average one proton is released per electron flow to ferricyanide on the electron acceptor side, consistent with the production of four protons by four-electron oxidation of two water molecules in the WOC. This result also clearly demonstrates that virtually all protons from the WOC were trapped by Mes molecules.

**Flash-Dependent Oscillation of Protein Bands.** The FTIR difference spectra upon individual flashes of the PSII core complexes in an unlabeled Mes buffer are presented in Figure 4. In these difference spectra, the Mes signals in the region below 1300  $\text{cm}^{-1}$  are relatively small compared with the protein signals that are mainly observed in the 1700–1300  $\text{cm}^{-1}$  region. The spectra of the S-state cycle in the protein region were basically identical to those previously reported for the core preparation from *T. elongatus*<sup>32,51</sup> and very similar to those for PSII preparations from other species.<sup>33,37,38,41,42,49</sup> The 1st, 2nd, 3rd, and 4th flash spectra (black lines) provide spectral features characteristic of the  $S_1 \rightarrow S_2$ ,  $S_2 \rightarrow S_3$ ,  $S_3 \rightarrow S_0$ , and  $S_0 \rightarrow S_1$  transitions, respectively.<sup>32,33,51</sup> The 5th–8th (red lines) and 9th–12th

(green lines) flash spectra showed features very similar to those of the 1st–4th flash spectra (black lines) but with smaller intensities. These observations indicate that protein reactions during the S-state cycle were unaffected by a relatively high concentration (200 mM) of a Mes buffer. It should be noted that signals typical of the  $Y_D^*/Y_D$  difference at 1705/1698  $\text{cm}^{-1}$ <sup>25,53</sup> and of the  $\text{Fe}^{2+}/\text{Fe}^{3+}$  difference at 1103  $\text{cm}^{-1}$ ,<sup>25,54,55</sup> which often contaminate the S-state spectra, were hardly observed in the spectra, indicating that the reactions of these species were suppressed by preflash illumination. The absence of  $Y_D$  signals was also confirmed by comparison with the S-state spectra of the core complexes from the  $Y_D$ -less mutant (D2-Y160F) of *T. elongatus*.<sup>56</sup>

The flash-number dependence of the intensity of the protein signal, which was evaluated by the intensity at 1400  $\text{cm}^{-1}$  relative to that at 1437  $\text{cm}^{-1}$ , the positions of the prominent symmetric carboxylate stretching peaks at the first flash, showed a clear period-four oscillation (Figure 4, inset). Simulation assuming a single miss factor (details of simulation are described in Supporting Information) provided a miss value of  $8.9 \pm 1.4\%$  (black open circles). A similar result was obtained for the spectra in Mes- $d_{12}$  with a miss factor of  $9.4 \pm 1.7\%$  (data not shown). This miss factor of  $\sim 9\%$  is similar or even better than the 12–13% misses in previous FTIR studies of the S-state cycle using the same core samples of *T. elongatus*.<sup>32,51</sup> Thus, it was again corroborated that the S-state cycling in the WOC properly took place in a high concentration Mes buffer.

**Proton Release Pattern Estimated by Mes Signals.** The intensities of isotope-edited Mes signals (Figure 2) were estimated by spectral fitting using a standard spectrum, which was obtained from the 12-flash spectrum (the largest spectrum in Figure 2) divided by 12 representing the Mes amount per one flash, in the 1282–1104  $\text{cm}^{-1}$  region that involved major Mes bands. The increase in the Mes intensity, i.e., the amount of protons, was plotted as a function of flash number in Figure 5 (red solid circles). Error bars express the standard deviations of the data obtained with four sets of experiments using different samples. A typical period-four oscillation with maxima at the 3rd, 7th, and 11th flash and with minima at the 1st, 5th, and 9th flash was observed.

This oscillation pattern of proton release was simulated with the equation described in the Supporting Information. There was a restriction that the sum of the numbers of protons released at the four transitions equals 4. The result of the first simulation in which a single miss factor was involved in fitting parameters (method 1) was depicted in Figure 5 (black open circles) superimposing the experimental data. The miss factor was estimated to be  $12 \pm 3\%$ , which is consistent with that of  $\sim 9\%$  estimated by protein bands (see above). The number of protons released in the  $S_0 \rightarrow S_1$ ,  $S_1 \rightarrow S_2$ ,  $S_2 \rightarrow S_3$ , and  $S_3 \rightarrow S_0$  transitions were estimated to be  $0.94 \pm 0.20$ ,  $0.28 \pm 0.11$ ,  $1.20 \pm 0.15$ , and  $1.57 \pm 0.16$ , respectively (Table 1). A similar pattern of

(51) Noguchi, T.; Sugiura, M. *Biochemistry* **2002**, *41*, 2322–2330.

(52) Hienerwadel, R.; Boussac, A.; Breton, J.; Diner, B. A.; Berthomieu, C. *Biochemistry* **1997**, *36*, 14712–14723.

(53) Takahashi, R.; Sugiura, M.; Noguchi, T. *Biochemistry* **2007**, *46*, 14245–14249.

(54) Hienerwadel, R.; Berthomieu, C. *Biochemistry* **1995**, *34*, 16288–16297.

(55) Noguchi, T.; Inoue, Y. *J. Biochem.* **1995**, *118*, 9–12.

(56) Suzuki, H.; Sugiura, M.; Noguchi, T. In *Photosynthesis. Energy from the Sun, 14th International Congress on Photosynthesis*; Allen, J. F., Gantt, E., Golbeck, J. H., Osmond, B., Eds.; Springer: Heidelberg, 2008; pp 513–516.

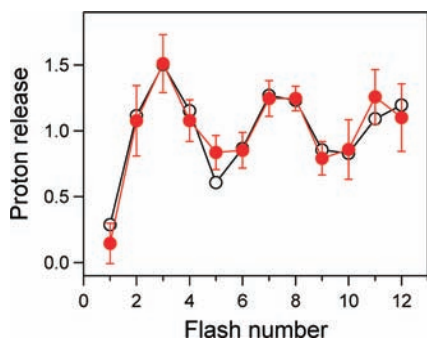


**Figure 5.** Proton release pattern as a function of flash number estimated by the intensity increase of the Mes signals (red closed circles). The error bars were evaluated as standard deviations of the data of four sets of experiments using different samples. The extent of proton release was expressed relative to the average proton release upon a single flash. The simulated pattern (black open circles) was obtained by fitting in which a single miss factor was included in fitting parameters in addition to the number of protons released at individual S-state transitions, providing a  $12 \pm 3\%$  miss and  $0.94 \pm 0.20$ ,  $0.28 \pm 0.11$ ,  $1.20 \pm 0.15$ , and  $1.57 \pm 0.16$  protons released in the  $S_0 \rightarrow S_1$ ,  $S_1 \rightarrow S_2$ ,  $S_2 \rightarrow S_3$  and  $S_3 \rightarrow S_0$  transitions, respectively.

$1.02 \pm 0.13$ ,  $0.33 \pm 0.10$ ,  $1.12 \pm 0.11$ , and  $1.53 \pm 0.12$  was obtained when the miss factor was fixed to 9% (method 2; Table 1).

The miss factors should be actually dependent on individual transitions, and thus the assumption of a single miss could affect the estimated values of proton release. De Wijn and van Gorkom<sup>57</sup> suggested from their fluorescence study that the miss of the  $S_3 \rightarrow S_0$  transition, in which molecular oxygen is released, is much larger than the other three transitions. Thus, an additional simulation was performed assuming that the miss of the  $S_3 \rightarrow S_0$  transition is twice as large as the misses of other transitions keeping the average miss factor of 9%, resulting in the misses of 14.4% in  $S_3 \rightarrow S_0$  and 7.2% in others (method 3). The proton release pattern was estimated to be  $0.99 \pm 0.13$ ,  $0.32 \pm 0.10$ ,  $1.09 \pm 0.10$ , and  $1.60 \pm 0.12$  in the  $S_0 \rightarrow S_1$ ,  $S_1 \rightarrow S_2$ ,  $S_2 \rightarrow S_3$ , and  $S_3 \rightarrow S_0$  transitions, respectively. Thus, the larger miss factor in the  $S_3 \rightarrow S_0$  transition only slightly increases the proton release in this transition, but the overall pattern was virtually unchanged.

**COOH Region of Carboxylic Groups of Proteins.** Figure 6b–e (black lines) show the C=O stretching region of protonated carboxylic groups (COOH) ( $1760\text{--}1700\text{ cm}^{-1}$ ) in the FTIR difference spectra upon the first (a), second (b), third (c) and fourth (d) flash illumination, which represent the  $S_1 \rightarrow S_2$ ,  $S_2 \rightarrow S_3$ ,  $S_3 \rightarrow S_0$ , and  $S_0 \rightarrow S_1$  transitions. Usually in proteins, this frequency region provides only COOH vibrations,<sup>59</sup> but in the PSII proteins, the C=O vibrations of ester groups of chlorophyll, pheophytin, and lipids can also appear in this region.<sup>50</sup> Several small but clear peaks were observed in each spectrum beyond the noise level that was revealed by a dark-minus-dark spectrum (a). Similarly to other protein bands (Figure 4), most of the peaks in the first and second flash spectra were reversed in the third and fourth flash spectra (indicated by blue dotted lines),<sup>32,51</sup> indicative of oscillating reactions or movements of COOH/ester groups in PSII proteins.

The C=O bands of COOH groups can be identified by  $7\text{--}20\text{ cm}^{-1}$  downshifts upon deuteration of exchangeable protons.<sup>58</sup> As a model compound of carboxylic side chains, the spectrum of protonated propionic acid (150 mM) in an aqueous solution (pH

2.7) in the presence of ferricyanide (15 mM) as an internal standard was measured (Figure 6f, black line). The spectrum in Figure 6f was scaled to express the formation of 0.5 COOH per reduction of one ferricyanide in PSII based on the CN peak of ferricyanide at  $2116\text{ cm}^{-1}$ , so that it is directly comparable to the S-state spectra (Figure 6b–e). A clear downshift by  $\sim 18\text{ cm}^{-1}$  was observed upon deuteration of the COOH hydrogen in  $D_2O$  solution (Figure 6f, red line).<sup>58</sup> The band intensity and the large deuteration shift of propionic acid demonstrate that the protonation/deprotonation reactions of carboxylic groups in PSII proteins should be detected if at least  $\sim 0.1\text{ H}^+$  is trapped by or released from carboxylic amino acids upon flash illumination, when taking into account the noise levels of the difference spectra (Figure 6a) being less than 0.2 of the COOH intensity. The features of the S-state spectra in the  $1760\text{--}1700\text{ cm}^{-1}$  region in a Mes/ $D_2O$  buffer (Figure 6b–e, red lines) were, however, basically identical to those in a Mes/ $H_2O$  buffer within the noise level. Thus, no bands of proton exchangeable COOH groups were identified in the FTIR spectra, and this result indicates that basically no proton release or uptake (less than  $\sim 0.1\text{ H}^+$ , if any) took place in carboxylic amino acids between S states. The bands in the  $1760\text{--}1700\text{ cm}^{-1}$  region may arise from COOH groups with nonexchangeable protons located in hydrophobic domains or ester groups electrostatically or structurally coupled to the WOC.

## Discussion

**FTIR Detection of Protons Released from the WOC.** In this study, we have monitored proton release during photosynthetic water oxidation by detecting infrared changes of Mes buffer molecules. To do so, we used a Mes buffer (pH 6.0) at a relatively high concentration (200 mM) to trap all protons released into a medium. From a  $pK_a$  of 6.15, 83 mM of Mes is expected to take a deprotonated form ( $\text{Mes}^-$ ; Figure 1C) in a 200 mM solution at pH 6.0. On the other hand, the PSII sample at a 10 mg of Chl/mL concentration used in the present experiment is estimated to involve 0.32 mM WOC, taking into account 35 Chls per one unit of the core complex of *T. elongatus*.<sup>6</sup> Application of a train of 12 flashes and 6 time repetitions for one sample will release 72 protons at maximum by water oxidation per one WOC. Thus, 23 mM protons should be released into the medium, all of which can be trapped by  $\text{Mes}^-$  (83 mM). In fact, the same number of Mes molecules as that of photoreduced ferricyanide was reacted (Figure 3d), indicating that virtually all protons from WOC were trapped by the Mes buffer without interference of the buffering effect of proteins. Thus, the number of protons released upon flash illumination can be correctly estimated using the intensity of the Mes bands.

Mes-only spectra without the contribution of protein bands were obtained by isotope-edited difference spectroscopy. Berthomieu and Hienelwadel<sup>25</sup> previously estimated the extent of proton uptake upon reduction of the nonheme iron in PSII using FTIR difference spectroscopy. They used different types of buffers to cancel the protein bands and obtain the buffer-only signals. In the case of water oxidizing reactions in the WOC, however, miss factors in the individual S-state transitions subtly affected by buffer species (data not shown), which hampered an accurate analysis of buffer bands. To circumvent this

(58) Takei, K.; Takahashi, R.; Noguchi, T. *J. Phys. Chem. B* **2008**, *112*, 6725–6731.

(59) Barth, A. *Biochim. Biophys. Acta* **2007**, *1767*, 1073–1101.

(57) de Wijn, R.; van Gorkom, H. J. *Photosynth. Res.* **2002**, *72*, 217–222.

**Table 1.** Number of Protons Released in the Individual S-State Transitions Estimated by Simulations of the Oscillation Pattern of the Mes Signal

	miss (%)	S <sub>0</sub> →S <sub>1</sub>	S <sub>1</sub> →S <sub>2</sub>	S <sub>2</sub> →S <sub>3</sub>	S <sub>3</sub> →S <sub>0</sub>
method 1 <sup>a</sup>	12 ± 3	0.94 ± 0.20	0.28 ± 0.11	1.20 ± 0.15	1.57 ± 0.16
method 2 <sup>b</sup>	9	1.02 ± 0.13	0.33 ± 0.10	1.12 ± 0.11	1.53 ± 0.12
method 3 <sup>c</sup>	7.2/7.2/14.4/7.2	0.99 ± 0.13	0.32 ± 0.10	1.09 ± 0.10	1.60 ± 0.12

<sup>a</sup> A single miss factor was included in fitting parameters. <sup>b</sup> The miss factor was fixed to 9% that was obtained from the oscillation pattern of protein bands. <sup>c</sup> The miss of the S<sub>3</sub>→S<sub>0</sub> transition was assumed to be twice that of other transitions keeping the average miss factor of 9%.

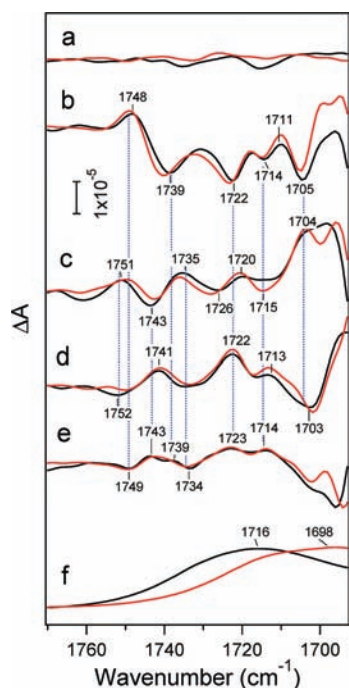


**Figure 6.** C=O stretching region of a carboxylic group (COOH) in the flash-induced FTIR difference spectra of the S-state cycle in a 200 mM Mes buffer (pH 6.0) (a–e) in comparison with that of a propionic acid solution (f). Black lines: in H<sub>2</sub>O; red lines: in D<sub>2</sub>O. Difference spectra of the S-state cycle were measured upon the first (b), second (c), third (d), and fourth (e) flash, representing the changes by the S<sub>1</sub>→S<sub>2</sub>, S<sub>2</sub>→S<sub>3</sub>, S<sub>3</sub>→S<sub>0</sub>, and S<sub>0</sub>→S<sub>1</sub> transitions, respectively. The dark-minus-dark difference spectra (a) show the noise levels of the difference spectra. Corresponding peaks are indicated by dotted lines. The aqueous solution of propionic acid (150 mM) contained potassium ferricyanide (15 mM) as an internal standard. The spectrum of H<sub>2</sub>O (or D<sub>2</sub>O) was subtracted from the spectra of propionic acid solutions. The intensity of the propionic acid spectrum was scaled to express the formation of 0.5 COOH per reduction of one ferricyanide in PSII based on the CN intensity of ferricyanide (2116 cm<sup>-1</sup>).

problem, we have measured the spectra in Mes-*d*<sub>12</sub>, which provided an S-state cycling identical to that in unlabeled Mes (Figure 1), to delete the protein bands from the spectra. The obtained isotope-edited Mes spectra (Figure 2) represented protons released from the WOC upon flash illumination.

**Proton Release Pattern.** The flash-number dependence of the proton release, which was estimated from the intensity increase of the Mes signals, showed a clear period-four oscillation (Figure 5). Simulations of these data with different assumptions about miss factors, i.e., a single miss factor involved in fitting parameters (method 1), the miss factor fixed to 9% obtained by protein bands (Figure 4, inset) (method 2), and the twice as large miss factor of the S<sub>3</sub>→S<sub>0</sub> transition than the misses of other transitions keeping an average miss of 9% (method 3), showed a similar proton release pattern of 0.9–1.0:0.2–0.3:1.0–1.2:1.5–1.6 for the S<sub>0</sub>→S<sub>1</sub>→S<sub>2</sub>→S<sub>3</sub>→S<sub>0</sub> transitions (Table 1). This proton release pattern is consistent with the previous result by Schlodder and Witt,<sup>23</sup> who reported a pattern of 1.0:

0.2:1.0:1.8 for a similar PSII core sample of *T. elongatus* at pH 6.0 from measurements using a pH glass electrode. The good agreement between the results by the two totally different methods using stable PSII core complexes that are crystallizable<sup>5,6,47</sup> implies that the obtained proton pattern is highly reliable. Similar patterns have also been observed for thylakoid membranes,<sup>18,22</sup> PSII membranes,<sup>17</sup> and core complexes stabilized with glycerol<sup>22</sup> at pH 6–7.

The above proton release pattern of *T. elongatus* core complexes is close to an integer pattern of 1:0:1:2 with some deviation at the S<sub>1</sub>→S<sub>2</sub> and S<sub>3</sub>→S<sub>0</sub> transitions. As a reason for this deviation, proton release/uptake by contaminating reactions of cofactors in PSII and electron acceptors is excluded. No evidence of contaminations of the Y<sub>D</sub><sup>\*</sup>/Y<sub>D</sub> (1705/1698 cm<sup>-1</sup>)<sup>52,53</sup> and Fe<sup>2+</sup>/Fe<sup>3+</sup> (1103 cm<sup>-1</sup>)<sup>25,54,55</sup> signals, which could release or uptake protons upon redox reactions,<sup>25,26</sup> was found in the FTIR difference spectra of the S-state transitions (Figure 4). Also, our preliminary proton release study using a Y<sub>D</sub>-less mutant (D2-Y160F) of *T. elongatus* showed a similar pattern of approximately 1.1:0.3:1.0:1.6.<sup>56</sup> Furthermore, we used ferricyanide as an electron acceptor instead of artificial quinones, which could disturb the proton pattern. The observation that the average number of released protons was identical to the number of reduced ferricyanide (Figure 3d) indicates that virtually all electron holes photogenerated in PSII were used for water oxidation.

The most plausible explanation for the observed proton release pattern is that the 1:0:1:2 pattern purely from substrate water is perturbed by partial protonation/deprotonation of amino acid groups nearby the WOC at the S<sub>1</sub>→S<sub>2</sub> and S<sub>3</sub>→S<sub>0</sub> transitions in response to the changes in the net charge at the Mn cluster, as suggested previously.<sup>11,23</sup> The contrasting idea is that protonation/deprotonation of amino acid groups that are strongly coupled to the S-state transitions significantly contributes to the approximate 1:0:1:2 pattern. In the latter case, dramatic pK<sub>a</sub> shifts of amino acid groups by S-state transitions must take place. Primary candidates for such amino acids are direct ligands to the Mn cluster. X-ray crystallographic structures of PSII proteins proposed 5–6 carboxylate groups and one His imidazole as ligands to the Mn cluster.<sup>5,6</sup> The present FTIR analysis in the COOH region (Figure 6), however, showed that no more than ~0.1 carboxylic groups per electron underwent protonation/deprotonation reactions upon S-state transitions. In addition, previous FTIR studies using [<sup>15</sup>N]His isotope labeling showed that the imidazole CN stretching peak at 1113 cm<sup>-1</sup> in the S<sub>2</sub>/S<sub>1</sub> FTIR difference spectrum was insensitive to H/D exchange<sup>36</sup> and no His bands were observed in the S<sub>0</sub>/S<sub>3</sub> difference spectrum.<sup>39</sup> Our preliminary data showed the His CN bands in the S<sub>3</sub>/S<sub>2</sub> and S<sub>0</sub>/S<sub>1</sub> transitions also did not show deuteration shifts (data not shown). Since deuteration of the imidazolium form of His (HisH<sup>+</sup>) induces a large upshift of the CN peak by

$\sim 20 \text{ cm}^{-1}$ ,<sup>60</sup> these data indicate that His side chains do not undergo protonation/deprotonation upon S-state transitions.

Thus, the FTIR analyses of proton release and protein reactions strongly suggest that protons are released from two water molecules with a 1:0:1:2 pattern for the  $S_0 \rightarrow S_1 \rightarrow S_2 \rightarrow S_3 \rightarrow S_0$  transitions and partial contributions of amino acid reactions disturb the integer values. This proton pattern is consistent with the net charge changes of  $0: +1: 0: -1$ <sup>61</sup> and the pH dependency of the transition efficiencies,<sup>62,63</sup> in which the  $S_1 \rightarrow S_2$  transition was pH independent, whereas the other three transitions were strongly inhibited at acidic pH values. Also, FTIR spectra of the weakly H-bonded water OH region showed negative bands, indicative of proton release or shifts to strong hydrogen bonds, in the  $S_2 \rightarrow S_3$ ,  $S_3 \rightarrow S_0$ , and  $S_0 \rightarrow S_1$  transitions, whereas the  $S_1 \rightarrow S_2$  transition showed a differential signal due to a minor change in the hydrogen bond intensity.<sup>43,44</sup> The negative band in the  $S_3 \rightarrow S_0$  transition has a twice larger intensity than the bands in other transitions, suggesting the reactions of two water OH bonds.

Amino acids responsible for partial protonation in the  $S_1 \rightarrow S_2$  transition and reprotonation in the  $S_3 \rightarrow S_0$  transition may be protonatable amino acids other than Asp, Glu, and His. Cys can also be excluded because no S–H peak was found in the typical S–H region of  $2600\text{--}2520 \text{ cm}^{-1}$  in the S-state FTIR spectra (data not shown). Hence, Arg, Lys, and Tyr are left as candidates. Indeed, CP43-Arg357 is located in the vicinity of the Mn cluster and was proposed to be directly involved in the reaction mechanism of water oxidation,<sup>64</sup> while D2-Lys317 is located  $\sim 7 \text{ \AA}$  away from the nearest Mn ion, interacting with  $\text{Cl}^{-47}$  that is indispensable for oxygen evolution. In addition, it could be possible that TyrZ (D1-Tyr160), which is a direct electron acceptor of the Mn cluster and usually protonated in its reduced state,<sup>65</sup> is partially deprotonated in some S states, although stable H-bonding with D1-His190<sup>5,6</sup> makes this situation rather unlikely. It is also less likely that nonspecific amino acid groups located remote from the WOC participate in proton release/uptake responding to the S-state transitions in the core complexes of *T. elongatus*, because virtually no protonation/deprotonation was detected in carboxylic groups (Figure 6), which are the most prominent in number among the protonatable groups in PSII proteins. Further detailed FTIR studies using selective isotope labeling of amino acids and site-directed mutagenesis will be necessary to specify the amino acid groups that are responsible for the partial proton release/uptake reactions.

**Implication in the Water-Oxidation Mechanism.** To date a number of models have been proposed for the mechanism of water oxidation.<sup>2,3</sup> They are based on structural information obtained by various methods such as X-ray crystallography, EXAFS, and  $^{18}\text{O}$  mass spectrometry, EPR, and FTIR. The proton release stoichiometry from substrate water is particularly crucial in constructing a proper model. Some of the models adopted the 1:1:1:1 pattern of proton release, which has been observed

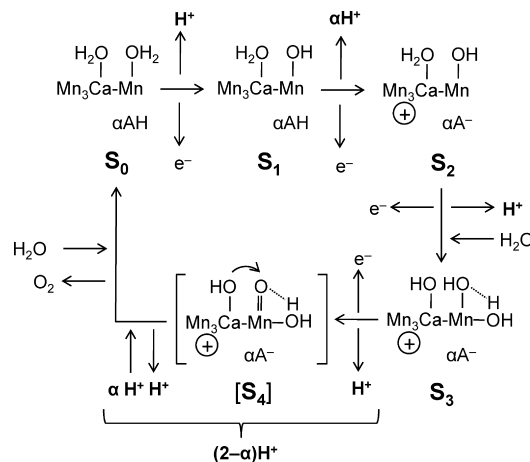


**Figure 7.** Schematic picture of the mechanism of water oxidation. The Mn cluster was expressed by a simplified model in which substrate water molecules are bound at the  $\text{Ca}^{2+}$  in the  $\text{Mn}_3\text{Ca}$  cluster and the dangling Mn in the  $S_0$  state. AH is a protonatable amino acid group near the Mn cluster. See text for details.

in core complexes of higher plants,<sup>15,20,22</sup> under the assumption that proton release from the smallest PSII unit capable of oxygen evolution should reveal a real pattern of proton release from the substrate. A typical one is the hydrogen abstraction model, in which TyrZ' abstracts a hydrogen atom from substrate water at each S-state transition.<sup>66</sup> On the other hand, other models mostly adopted the 1:0:1:2 pattern that was originally proposed from the data of thylakoids.<sup>2,3</sup> The result in the present FTIR study using robust core complexes of *T. elongatus* strongly supported this 1:0:1:2 pattern, thus the former models can be dismissed. In addition, significant contributions of amino acid ligands to proton release or uptake are unnecessary to consider, while minor contributions of nearby amino acid groups, perhaps the side chains of Arg, Lys, or Tyr, are involved in the reaction.

A schematic picture of the water oxidation mechanism is presented in Figure 7 to illustrate the view obtained in the present study. The X-ray crystallographic structures of the PSII core complexes indicated that the Mn cluster has a "3 + 1" structure consisting of a  $\text{Mn}_3\text{Ca}$  cluster and a dangling Mn.<sup>5,6</sup> Recent sophisticated models<sup>67,68</sup> proposed by density functional theory calculations based on the X-ray structure demonstrated that the  $\text{Ca}^{2+}$  and the dangling Mn ions play a critical role in substrate reactions. However, the binding and reactions of substrates are not so simple in these models; several water or hydroxide ligands are bound to the Mn cluster and oxo- or hydroxo-bridges are significantly involved in the reactions. For simplicity, the present scheme in Figure 7 starts with two water molecules bound to the  $\text{Ca}^{2+}$  and the dangling Mn in the  $S_0$  state. Nearby the Mn cluster, there is a protonatable amino acid group (AH), whose  $\text{pK}_a$  is affected by the change in the net charge of the Mn cluster including substrate intermediates. In the  $S_0 \rightarrow S_1$  transition, one proton is released from substrate water without a change in the net charge, whereas in the  $S_1 \rightarrow S_2$  transition, in which there is no proton release from substrate, one positive charge is accumulated on the Mn cluster. This charge increase causes a downshift of the  $\text{pK}_a$  of the nearby amino acid, resulting in its partial proton release. During the

(60) Hasegawa, K.; Ono, T.; Noguchi, T. *J. Phys. Chem. B* **2000**, *104*, 4253–4265.

(61) Saygin, O.; Witt, H. T. *FEBS Lett.* **1984**, *176*, 83–87.

(62) Bernát, G.; Morvaridi, F.; Feyziyev, Y.; Styring, S. *Biochemistry* **2002**, *41*, 5830–5843.

(63) Suzuki, H.; Sugiura, M.; Noguchi, T. *Biochemistry* **2005**, *44*, 1708–1718.

(64) McEvoy, J. P.; Brudvig, G. W. *Phys. Chem. Chem. Phys.* **2004**, *6*, 4754–4763.

(65) Berthomieu, C.; Hienerwadel, R.; Boussac, A.; Breton, J.; Diner, B. A. *Biochemistry* **1998**, *37*, 10547–10554.

(66) Hoganson, C. W.; Babcock, G. T. *Science* **1997**, *277*, 1953–1956.

(67) Sproviero, E. M.; Gascon, J. A.; McEvoy, J. P.; Brudvig, G. W.; Batista, V. S. *J. Am. Chem. Soc.* **2008**, *130*, 3428–3442.

(68) Siegbahn, E. M. *Chem.—Eur. J.* **2008**, *14*, 8290–8302.



S<sub>2</sub>→S<sub>3</sub> transition, another proton is released without a change in the net charge. One water molecule may be inserted in this step according to our FTIR results of dehydration effects on transition efficiencies and the analysis of the DOD bending vibrations.<sup>45,51</sup> This water does not necessarily function as a substrate in this S-state cycle but could assist the reaction through a hydrogen bond interaction and will become a substrate in the next cycle. Upon formation of the transient S<sub>4</sub> state from the S<sub>3</sub> state, the release of one proton generates a terminal Mn=O or Mn–O\*, which will undergo a nucleophilic attack by hydroxide or water to form an O–O bond.<sup>2,3</sup> The S<sub>4</sub> state relaxes to the initial S<sub>0</sub> state by releasing a proton to produce an oxygen molecule. The net charge decreases in this step, and the nearby amino acid is reprotonated by partial proton uptake. Thus, the sum of protons released into bulk during the S<sub>3</sub>→[S<sub>4</sub>]→S<sub>0</sub> transition becomes smaller than 2.

### Conclusion

We have successfully detected protons released from the WOC during water oxidation in PSII core complexes of *T. elongatus* by means of isotope-edited FTIR difference spectroscopy. In combination with the analysis of protein bands in FTIR difference spectra, it was concluded that proton release from substrate water takes place with a 1:0:1:2 pattern for the

S<sub>0</sub>→S<sub>1</sub>→S<sub>2</sub>→S<sub>3</sub>→S<sub>0</sub> transitions, which is slightly perturbed by protons from amino acid groups near the Mn cluster probably other than carboxylic groups, His imidazole, and Cys S–H. The results of the present study demonstrate that FTIR difference spectroscopy that provides simultaneous analyses of proton release/uptake and protein and cofactor reactions is fruitful for studies not only of water oxidizing reaction but also of other protolytic reactions in many enzymes. Further FTIR studies of proton release during water oxidation at different pH's and materials, which have been showing controversial results in previous studies,<sup>8,9</sup> will provide a definite conclusion on the proton release mechanism in photosynthetic water oxidation.

**Acknowledgment.** This study was supported by Grants-in-Aid for Scientific Research (17GS0314) from the Ministry of Education, Culture, Sports, Science and Technology to T.N. and Grant-in-Aid for JSPS Fellows (19252) to H.S.

**Supporting Information Available:** The methods of simulations of the oscillation patterns of protein bands and proton release. This material is available free of charge via the Internet at <http://pubs.acs.org>.

JA901696M